Eu-doped barium aluminium oxynitride with the ß-alumina-type structure as new blue-emitting phosphor

Journal of The Electrochemical Society, **146** (2) 800-806 (1999)
S0013-4651(98)05-045-9 CCC: $7.00

Eu-Doped Barium Aluminum Oxynitride with the β-Alumina-Type Structure as New Blue-Emitting Phosphor

S. R. Jansen,[a] J. M. Migchels,[b] H. T. Hintzen,[z] and R. Metselaar

Laboratory of Solid State and Materials Chemistry, Centre for Technical Ceramics, Eindhoven University of Technology, 5600 MB Eindhoven, The Netherlands

Attractive new blue-emitting phosphors for use in low-pressure mercury gas discharge lamps are synthesized by Eu-substitution in the barium aluminum oxynitride host lattice with the β-alumina-type structure. The emission spectra of these phosphors for 254 nm excitation show a band at about 450 nm with a shoulder at higher wavelength. The maximum quantum efficiency of these materials is about 85-90% just like commercial $BaMgAl_{10}O_{17}$:Eu with the β-alumina type structure. The nonoptimized oxynitride phosphors are more sensitive to oxidation (at 873 K) and to short-term depreciation due to 185 nm irradiation compared to commercial $BaMgAl_{10}O_{17}$:Eu. However, the maintenance of the oxynitride phosphors in single component fluorescent lamps is improved. Calculations indicate that by using these phosphors in tricolor fluorescent lamps instead of $BaMgAl_{10}O_{17}$:Eu with the β-alumina type structure, the color rendering index will improve while the lumen output remains high.

Manuscript received May 15, 1998.

Fluorescent lamps are very important lighting sources since they have a high efficiency, a good color rendering, adjustable color temperature, and a long lifetime. It was predicted by Koedam and Opstelten[1] as well as by Thornton[2] that a fluorescent lamp with a high efficacy and color rendering index (CRI) can be obtained by combining three phosphors which emit in narrow wavelength intervals centered around 450 (blue), 550 (green), and 650 (red) nm. Such a lamp was realized a few years later, based on rare-earth activated phosphors and is called the tricolor lamp.[3]

A commonly used blue-emitting phosphor in tricolor lamps with a CRI of about 85 is Eu^{2+}-doped $BaMgAl_{10}O_{17}$. [3-5] The material $BaMgAl_{10}O_{17}$ has the β-alumina-type structure (space group $P6_3/mmc$) and can be derived from sodium β-alumina by replacing $(NaAl)^{4+}$ with $(BaMg)^{4+}$. So substituting Al^{3+} by Mg^{2+} is necessary for charge compensation when Na^+ is substituted by Ba^{2+}.

In the BaO-Al_2O_3 system such a charge compensation is not possible, so the β-alumina material observed in this system has a defect structure. The material is named barium aluminate phase I and has an ideal composition of $Ba_{0.75}Al_{11}O_{17.25}$. In this case Na^+ is substituted by $(Ba_{0.75}O_{0.25})^+$ and the defects in this structure are called Reidinger defects. These Reidinger defects consist of a Ba vacancy, an O interstitial, and two Al Frenkel defects. The exact composition of Ba aluminate phase I is not clear since the reported composition of this material ranges from a Ba/Al ratio of 0.058 to 0.094.[6-21] Also the Eu^{2+}-doped Ba β-alumina's are important luminescent materials and are therefore studied extensively.[3,6,22-32] $BaMgAl_{10}O_{17}$ is strongly related to Ba aluminate phase I since a solid solution exists between both materials.[25]

A novel way for obtaining a stoichiometric barium β-alumina is to realize charge compensation by the replacement of O^{2-} by N^{3-}. This results in the compound $BaAl_{11}O_{16}N$, [33] which also forms a solid solution with Ba aluminate phase I as has been proven by us recently.[34] Because of the importance of Eu-doped Ba β-alumina's as phosphors it is interesting to know what the luminescence properties are of Eu-doped $BaAl_{11}O_{16}N$.

In the present study we deal with Eu^{2+}-doped $BaAl_{11}O_{16}N$ for application as a phosphor in a low-pressure mercury gas discharge lamp. The properties of this material will be compared with Eu-doped Ba aluminate phase I and commercial Eu-doped $BaMgAl_{10}O_{17}$.

Some important qualifications of phosphors for application in a low-pressure mercury gas discharge lamp are

1. Small particle size and a narrow particle size distribution.—The particle size has to be small in order to result in a solid attachment between the powder and the glass of the lighting tube. However, to prevent severe scattering of UV-radiation which results in a low UV-absorption, the average particle size has to be larger than 2 μm with the fraction of particles smaller than 2 μm as small as possible.

2. High UV-absorption.—This means that the 254 nm radiation has to be absorbed efficiently, since this is the most important radiation in a low-pressure mercury gas discharge lamp.

3. High quantum efficiency.—The absorbed UV-radiation has to be converted efficiently into visible radiation, and nonradiative return to the ground state has to be minimal.

4. No oxidation in air below 873 K.—During the lamp-making process this temperature is used to remove the organic binder and the suspension medium.

5. Limited depreciation in the lamp during operation.—The phosphor has to be stable in the lamps to guarantee a long lifetime. Usually the phosphor degrades during lamp life, resulting in a decreased lumen output, possibly combined with a shift of color. The most important processes causing this declination are[5] (*i*) drop in quantum efficiency due to photochemical decomposition by 185 nm radiation from the mercury gas discharge; (*ii*) formation of absorbing layers due to reaction with excited mercury atoms from the gas discharge; and (*iii*) diffusion of sodium ions from the glass.

6. The color rendering index of the tricolor lamp should be high.[35]—A high CRI means that objects illuminated by the tricolor lamp or natural light appear similar to the human eye.

Experimental

Synthesis.—Several starting mixtures were made by combining the appropriate amounts of $BaCO_3$ (Merck, >99%), Eu_2O_3 (Rhône-Poulenc, 99.99%), $MgCO_3$ (Riedel-de Haen, >99%), AlN (Starck grade C, >97%), and γ-Al_2O_3 (Sumitomo AKPG, >99.995%). Corrections were made for weight losses and the amount of AlN is corrected for its oxygen content by taking it into account as Al_2O_3. The choice of γ-Al_2O_3 starting material is based on its high reactivity.[36] The general composition of the samples is

$$Eu_{x(0.83+0.17y)}Ba_{(1-x)(0.83+0.17y)}Al_{11}O_{(17.33-1.33y)}N_y$$

with x: 0, 0.01, 0.05, 0.10, 0.15, 0.40, 0.70, and 1.00 and y: 0, 0.17, 0.55, and 1.

We also prepared a magnesium-containing sample with the composition of $Eu_{0.1}Ba_{0.9}MgAl_{10}O_{17}$.

The powders were wet-mixed in isopropanol (>97%) for 2 h in an agate container with agate balls on a planetary mill. After mixing the isopropanol was evaporated. The powders were dried in a stove for one night at 433 K and subsequently ground in an agate mortar.

[a] Present address: Philips Lighting Division, 5600 JM Eindhoven, The Netherlands.
[b] Present address: Océ-Technologies, 5900 MA Venlo, The Netherlands.
[z] E-mail: tgtvbh@chem.tue.nl

S0013-4651(98)05-045-9 CCC: $7.00

The powders were fired in a molybdenum crucible under a mildly flowing N_2/H_2 (90/10) gas mixture. Reactions were performed in a vertical high-temperature tube furnace at 1973 K for 2 or 4 h (heating/cooling rate 3 K/min). $Eu_{0.1}Ba_{0.9}MgAl_{10}O_{17}$ is fired for 4 h at 1973 K.

The properties of the synthesized powders are compared with commercial Eu^{2+}-doped $BaMgAl_{10}O_{17}$ (Philips Lighting, U716), which contains about 10% Eu. In this work we refer to this commercial material as BAM.

Characterization

The phases, present after reaction, were determined by powder X-ray diffraction (XRD). Continuous scans were made with Cu Kα radiation from 5 to 75° (2θ), with a scan speed of 1° (2θ)/min (Philips 5100). Step scans, with a step size of 0.01° (2θ) and a counting time of 6 s/step, were made from 68 to 75° (2θ) in order to determine the presence of traces of AlN. For Eu-containing specimens, Fe Kα radiation was used instead of Cu Kα, to prevent fluorescence which increases the noise of the spectra. The lattice parameters were calculated by using the following reflections: 2 0 14, 2 2 0, 2 0 13, 3 0 4, 2 0 11, 2 1 7, 1 0 11, 1 1 8, 2 0 6, 2 0 5, and 1 0 10.

The powder morphology was studied by scanning electron microscopy (SEM), JEOL-840A. The powder samples were suspended in isopropanol and droplets were put on a brass sample holder. After evaporation of the isopropanol, a thin gold layer was sputtered on the samples to avoid charging.

The particle size and distribution was determined with a laser diffraction system, CILAS HR 850.

Luminescence

The luminescence measurements were performed at room temperature, using three kinds of spectrophotometers. The first type is a Perkin-Elmer LS50B spectrophotometer with a xenon flash lamp. The lamp spectrum is corrected with a double photomultiplier. The second type is a SPEX spectrophotometer, using a deuterium lamp. For both spectrophotometers the emission spectra are recorded using excitation radiation with a wavelength of 254 nm. Furthermore, the excitation spectrum was measured at the emission wavelength with maximum emission intensity ($\lambda_{em,max}$).

Reflection measurements were recorded on the SPEX spectrophotometer. The reflection spectrum of $BaSO_4$ is used for calibration by using the following data for its reflection: 250 nm excitation 95%, 300 nm 96.8%, 350 nm 97.8%, 400 nm 98.7%, 500 nm 99.1%, and 700 nm 99.2%.

The amount of UV-absorption at 254 nm was determined by measuring the diffuse reflection of semi-infinite powder layers at 254 nm, using the third spectrophotometer: the FLAME-1 apparatus of Philips Lighting. The measurement was calibrated using $CaCO_3$ (80% reflection) and using a black sample (3% reflection).

The second important feature determined with the FLAME-1 apparatus is the quantum efficiency. This is defined by the ratio of the number of emitted visible photons and the number of UV-photons absorbed by the phosphor. The quantum efficiency (*QE*) is calculated by relating the emitted radiation intensity of the sample integrated over the complete wavelength range to the emitted radiation intensity of a standard phosphor, Mn-doped Zn_2SiO_4 (Willemite) with a quantum efficiency of 80% at 254 nm, and multiplying this with the ratio of the UV-absorption of the standard and the sample

$$QE = \frac{\text{UV - absorption}_{\text{standard}}}{\text{UV - absorption}_{\text{sample}}} \cdot \frac{\text{Intensity emission}_{\text{sample}}}{\text{Intensity emission}_{\text{standard}}} \cdot QE_{\text{standard}} \quad [1]$$

To test the oxidation behavior the phosphor powders were put for 10 min in an oven at 873 K in air. Before and after this treatment the quantum efficiency, UV-absorption, and emission spectra were measured. Furthermore, combined differential thermal analysis and thermogravimetric analysis (DTA/TGA) were performed in air using a Netzsch STA 409. A heating rate of 5 K/min is applied to a maximum temperature of 1073 K.

The short-term depreciation (*STD*) in fluorescent lamps is simulated by measuring the light output of the phosphor when the phosphor is excited during a few minutes with both 185 and 254 nm radiation in the correct ratio. A correction was performed for the background signal by using a nonemitting black sample as standard. The *STD* is calculated using the following formula

$$STD = \frac{(\text{lumen output}_{0\,\text{minutes}} - \text{lumen output}_{6\,\text{minutes}})_{\text{sample}}}{(\text{lumen output}_{0\,\text{minutes,samples}} - \text{lumen output}_{\text{standard}})} \cdot 100\% \quad [2]$$

Single-component lighting tubes (2.6 mm diam) are prepared with three types of phosphors ($Eu_{0.09}Ba_{0.83}Al_{11}O_{16.59}N_{0.55}$, $Eu_{0.14}Ba_{0.78}Al_{11}O_{16.59}N_{0.55}$, and commercial BAM). Coating weight of the phosphors is 2.9 mg/cm^2, resulting in a layer thickness of about 17 μm. The median diameter of the powders used is 5.3 μm. Changes in emission color and lumen output of the prepared lamps are measured in time. Because a small tube diameter is used, the wall load is high. Therefore an indication of long range maintenance results was obtained in a relatively short amount of time (40, 80 h), assuming that the degradation mechanism of the phosphor does not change by applying a high wall load. The measured lamp spectra of these lighting tubes were used to calculate the theoretical CRI of a tricolor lamp by the Philips simulation program PHOCAL.

Results and Discussion

Powder characterization.—In our previous work we have shown that the *c*/*a* ratio is a reliable measure for observing the incorporation of nitrogen in Ba β-alumina.[33,34] According to XRD measurements the unit cell dimensions change (*a* increasing, *c* decreasing) with increasing nitrogen content, resulting in a decreasing *c*/*a* ratio as is shown in Fig. 1 for samples doped with Eu ($x = 0.1$). This phenomenon was observed previously for samples without Eu, so it can be concluded that it is possible to incorporate nitrogen.[33,34]

The shape of the *c*/*a* curve for samples with Eu ($x = 0.1$) is comparable to the curve reported for samples without Eu fired at 1973 K.[33,34] Only the absolute *c*/*a* values appear to be somewhat lower. Therefore we have determined the influence of the Eu-incorporation on the *c*/*a* ratio. The *c*/*a* ratio of both Eu-doped Ba aluminate phase I and $BaAl_{11}O_{16}N$ is decreasing with increasing Eu content (see Fig. 2), which is expected since the ionic radius of Eu^{2+} is smaller than that of Ba^{2+}.[37] At Eu-contents of $x = 0.4$ and higher $EuAl_{12}O_{19}$, with the magnetoplumbite-type structure (*c*/*a* ratio of 3.953), is observed as a secondary phase. This indicates that the

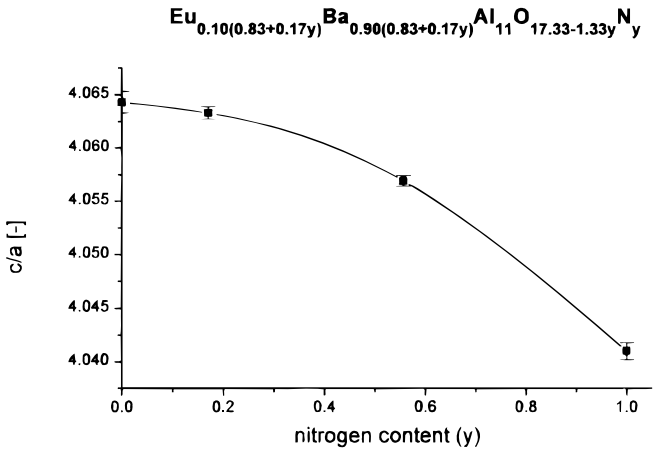

Figure 1. *c*/*a* ratio as a function of the nitrogen content (*y*) in Ba aluminum oxynitride with the β-alumina-type structure doped with Eu ($x = 0.1$) and fired at 1973 K for 2 h.

S0013-4651(98)05-045-9 CCC: $7.00

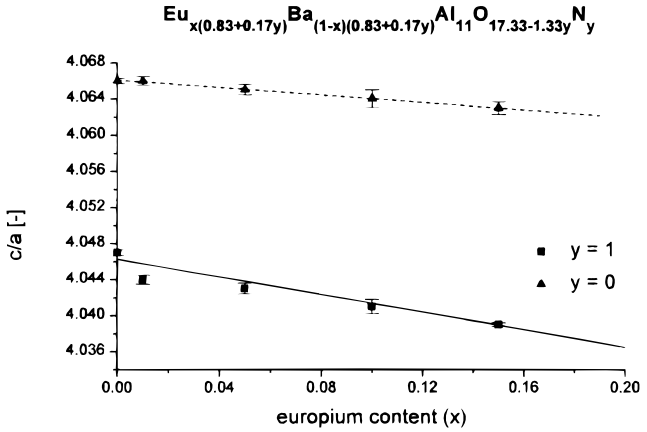

Figure 2. *c*/*a* ratio vs. europium content (*x*) in Eu-doped Ba aluminate phase I ($y = 0$) and $BaAl_{11}O_{16}N$ ($y = 1$). The samples were fired at 1973 K for 2 h.

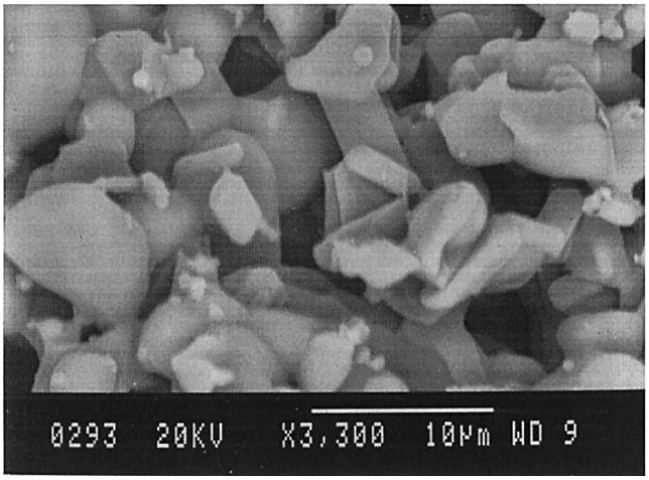

Figure 3. SEM photograph of $Eu_{0.1}Ba_{0.9}Al_{11}O_{16}N$ powder phosphor synthesized at 1973 K for 2 h.

maximum percentage of Eu-incorporation in Ba β-alumina is in between $x = 0.15$ and 0.4.

Scanning electron microscopy (SEM) pictures reveal that the powders of all Eu-doped Ba β-alumina's consist of hexagonal shaped platelets (Fig. 3 and 4). The powder morphology of the commercial powder BAM is more regularly shaped (Fig. 4) and seems to

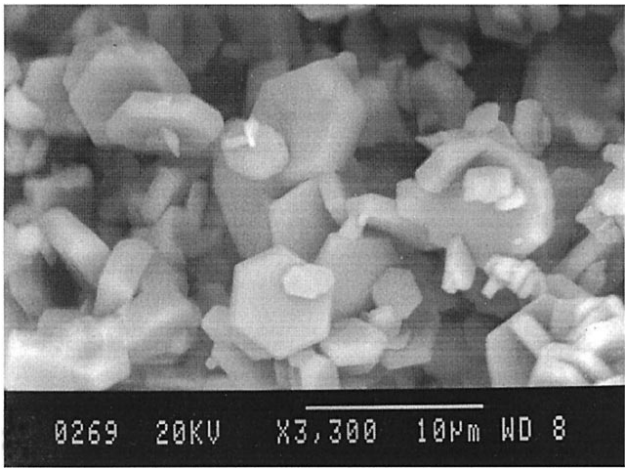

Figure 4. SEM photograph of commercial BAM powder phosphor.

have a more uniform grain size distribution compared to the samples synthesized in this work.

As expected on the basis of the SEM pictures the grain size distribution of commercial BAM is indeed narrower than of the other Eu-doped Ba β-alumina powders (Fig. 5). These differences are ascribed to fluxes, used in the synthesis of commercial BAM to obtain a more uniform powder morphology, and that after-treatment was applied to obtain a narrower grain size distribution.

Luminescence properties.—The luminescence properties are only determined for the single-phase materials but not for the samples with high Eu-concentrations ($x = 0.4$, 0.7, and 1.0).

In Fig. 6 the emission and excitation spectra are shown of Ba aluminate phase I, $BaAl_{11}O_{16}N$, and $BaMgAl_{10}O_{17}$ substituted with Eu ($x = 0.1$). In all emission spectra of the samples fired for 2 h at 1973 K, except for commercial BAM, a very small amount of Eu^{3+} emission (around 610 nm) is observed. This indicates that Eu^{3+} from the Eu_2O_3 starting material is not yet completely reduced to Eu^{2+}.

The most striking difference in the emission spectra is the presence of a shoulder in Eu-doped Ba aluminate phase I and $BaAl_{11}O_{16}N$ and the absence of this shoulder in the spectrum of Eu-doped $BaMgAl_{10}O_{17}$ (Fig. 7). This is in accordance with our previous results.[38] The differences in emission spectra between Eu-doped Ba aluminate phase I and $BaMgAl_{10}O_{17}$ were reported earlier.[23] It is clear from Fig. 6 that the luminescence behavior of Eu-doped Ba aluminate phase I and $BaAl_{11}O_{16}N$ is only slightly different. This indicates that nitrogen is not coordinated to europium which we have indeed proved by neutron diffraction.[39] The significant influence of

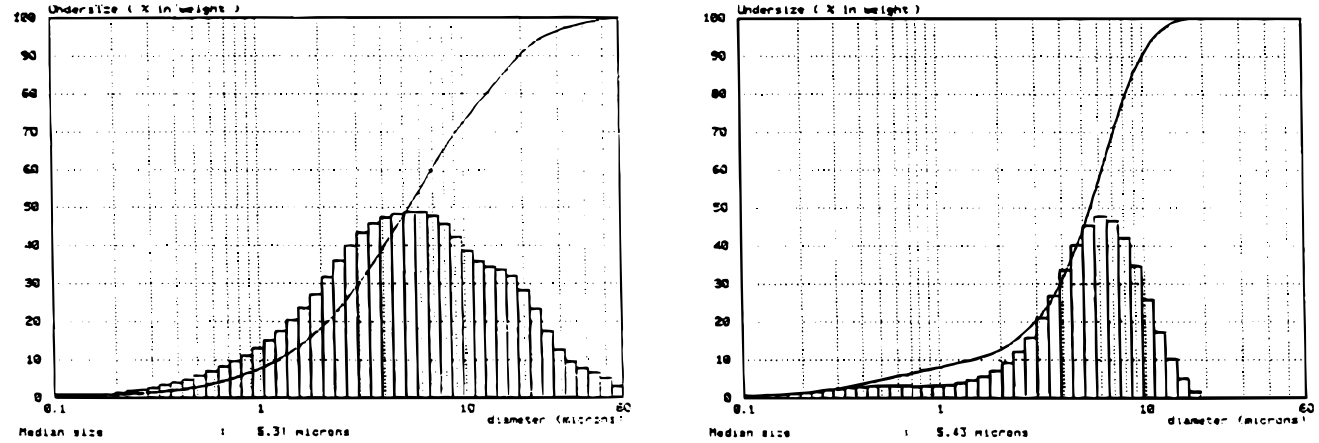

Figure 5. Particle size distribution, as observed by laser diffraction, of $Eu_{0.092}Ba_{0.833}Al_{11}O_{16.59}N_{0.55}$ synthesized at 1973 K for 4 h (left) and commercial BAM (right).

S0013-4651(98)05-045-9 CCC: $7.00

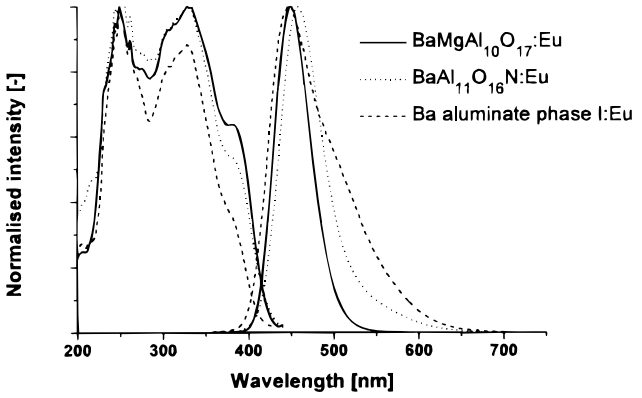

Figure 6. Emission spectra for 254 nm excitation and excitation spectra (at emission wavelength with maximum intensity) of various Ba β-alumina's substituted with Eu ($x = 0.1$), fired at 1973 K for 4 h.

coordination with N^{3-} ions was shown for a similar luminescent ion (Ce^{3+}) in Y-Si-O-N host lattices.[40] The presence of the shoulder indicates the presence of two Eu-sites in Eu-substituted Ba aluminate phase I and $BaAl_{11}O_{16}N$. In a subsequent paper we focus on the luminescence properties of the two Eu sites in $BaAl_{11}O_{16}N$ and the possibility of energy transfer between them and compare this to Ba aluminate phase I and $BaMgAl_{10}O_{17}$. [41]

The emission wavelength at maximum intensity of Eu-doped Ba aluminate phase I shifts to higher wavelengths with increasing europium content (Fig. 7), which is caused by an extended intensity of the shoulder. The emission wavelength of maximum intensity of Eu-doped $BaAl_{11}O_{16}N$ only increases for low Eu concentrations.

As expected, the UV-absorption becomes larger with increasing europium content approaching an asymptotic value of about 90% (Fig. 8). The UV-absorption of the Eu-doped samples fired for 4 h is higher than that of Ba aluminate phase I and $BaAl_{11}O_{16}N$ with the same Eu concentration of $x = 0.1$ which are fired for 2 h. This is ascribed to the longer firing time (4 h instead of 2 h) resulting in a slightly higher particle size. The UV-absorption of commercial BAM is higher, which is caused by the smaller fraction of grains below 2 μm. In the laboratory-made powders a significant number of the particles is smaller than 2 μm resulting in a lower UV-absorption due to increased scattering.

From the measured UV-absorption (A), the ratio of absorption coefficient (a) and scattering coefficient (s) was calculated using the Kubelka-Munk formula[42]

$$\frac{a}{s} = \frac{A^2}{2\cdot(1 - A)} \qquad [3]$$

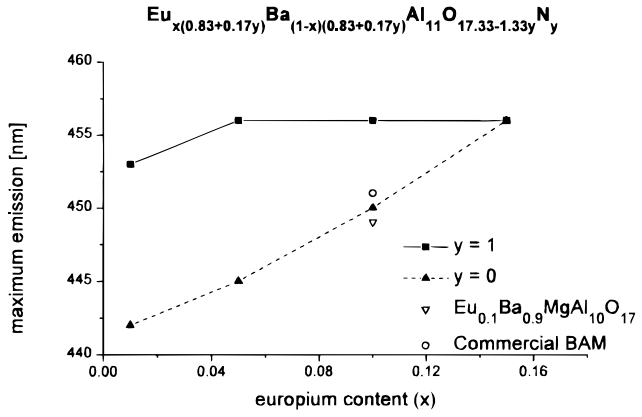

Figure 7. Emission wavelength at maximum intensity of Eu-doped Ba β-alumina's as a function of the europium content (x). The samples are fired for 2 h at 1973 K, only $Eu_{0.1}Ba_{0.9}MgAl_{10}O_{17}$ is fired for 4 h.

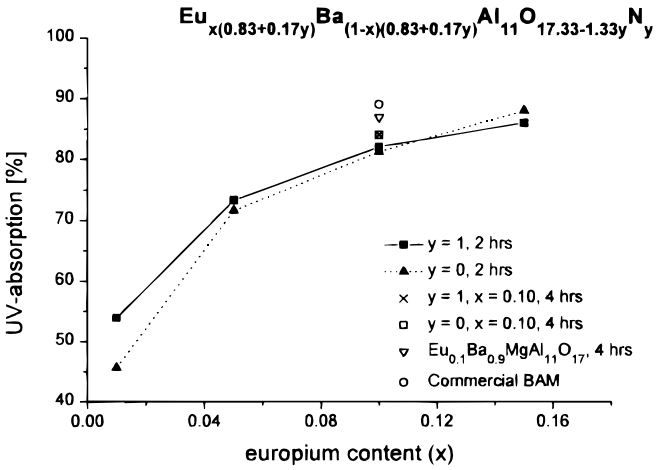

Figure 8. UV-absorption (254 nm) of various Eu-doped Ba β-alumina's as a function of the europium content (x).

As expected from the Lambert-Beer law for direct excitation of the Eu center, the calculated ratio between the absorption coefficient and scattering coefficient of Eu-doped Ba aluminate phase I is linearly dependent on the europium content and intersects the zero point (Fig. 9). However, the linear curve of the a/s ratio for Eu-doped $BaAl_{11}O_{16}N$ does not intersect the zero point but crosses the y axis at a value of about 0.15 (Fig. 9). This is caused by the host-lattice absorption. The a/s value of $x = 0.01$ is about 0.3 for Eu-doped $BaAl_{11}O_{16}N$, indicating that at this concentration about half of the photons is absorbed by the host-lattice ($a/s = 0.15$) followed by non-radiative losses. This corresponds very well with the quantum efficiency for this material that is also about half of the maximum value observed for Eu-doped $BaAl_{11}O_{16}N$ (Fig. 10).

The large a/s ratio of $Eu_{0.1}Ba_{0.9}MgAl_{10}O_{17}$ and commercial BAM is ascribed to the larger particle size of these powders, resulting in a smaller scattering coefficient and thus in a larger a/s ratio when the same a is assumed. This also holds for the Eu-doped powders with $y = 0$ and $y = 1$ as is shown in Fig. 9.

In general all samples show high quantum efficiencies (Fig. 10). The nitrogen concentration does not influence the quantum efficiency at high europium concentrations: all oxynitride samples with varying nitrogen content and substituted with $x = 0.1$ Eu have a quantum efficiency around 80% for samples fired for 2 h and about 85% for samples fired for 4 h (Table I). As is shown in Fig. 10, the

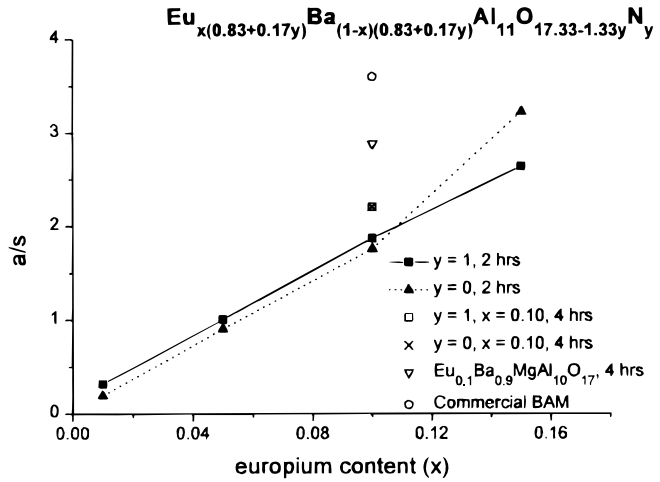

Figure 9. The ratio of the absorption coefficient and the scattering coefficient (a/s, at 254 nm) of various Eu-doped Ba β-alumina's as a function of the europium content (x).

S0013-4651(98)05-045-9 CCC: $7.00

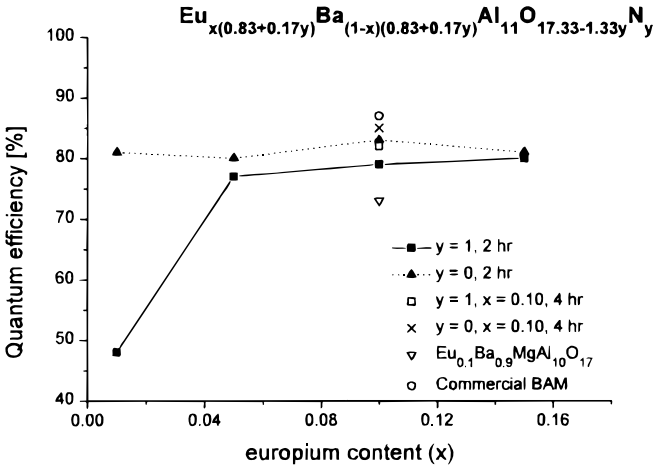

Figure 10. Quantum efficiency of various Eu-doped Ba β-alumina's as a function of the europium content (x).

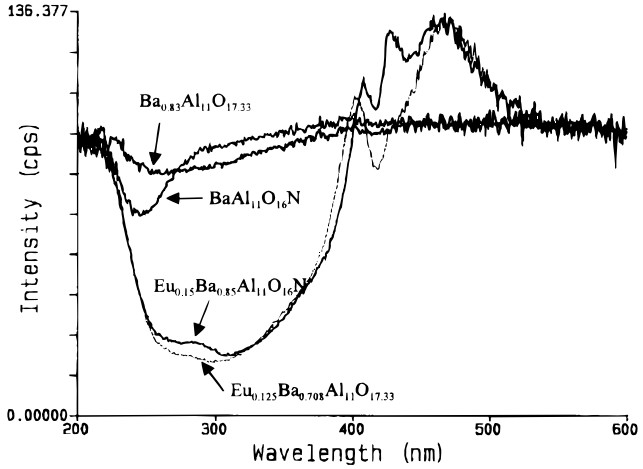

Figure 11. Reflection spectra showing competitive absorption around 250 nm in $BaAl_{11}O_{16}N$.

quantum efficiency of $BaAl_{11}O_{16}N$: Eu is reduced at low Eu contents. This might be caused by the presence of host-lattice absorption in $BaAl_{11}O_{16}N$ as is shown by reflection measurement (Fig. 11). The quantum efficiency of $Eu_{0.1}Ba_{0.9}MgAl_{10}O_{17}$ is lower compared to Ba aluminate phase I and $BaAl_{11}O_{16}N$ with $x = 0.1$ Eu. The quantum efficiency of commercial BAM is higher compared to the materials which are fired for 2 h. It is interesting to note that the quantum efficiency of samples fired for 4 h is already equivalent to commercial BAM, while these phosphors are not optimized indicating that even better values can be expected. Up to $x = 0.15$ no concentration quenching of the luminescence occurs.

Increasing the firing time from 2 to 4 h at 1973 K improves the quantum efficiency and UV absorption for the oxynitride phosphors (Table I), making the values comparable to those of commercial BAM. An increase of the particle size due to the longer firing time is expected, which results in a smaller scattering coefficient *s* and therefore in a larger UV-absorption *A* (see Eq. 3). The improved quantum efficiency is ascribed to a better crystallinity of the host-lattice and to a full reduction of Eu^{3+} to Eu^{2+}, since Eu^{3+} emission is diminished after 4 h at 1973 K.

The influence of the oxidation test on the quantum efficiency, UV-absorption, and emission wavelength with maximum intensity is given in Table II. It is clear that the quantum efficiency of the samples containing nitrogen is decreased after the oxidation test, while the quantum efficiency of the other samples is unaffected. This indicates that the nitrogen containing samples are somewhat affected by the heat-treatment in air. Since no weight losses nor peaks are observed in TGA and DTA measurements, it can be concluded that the amount of bulk oxidation is negligible. However the limited oxidation is strong enough to influence the quantum efficiency and the emission color of the samples. According to the available literature the related oxynitride $LnAl_{12}O_{18}N$ (Ln = La, Ce, Nd, Pr, Sm, and Gd) does not oxidize below 973 K.[43]

All samples, except commercial BAM, show short-term depreciation (*STD*) (Table III). The *STD* increases with increasing nitrogen content of the samples. An additional *STD* test on $Eu_{0.15}Ba_{0.85}Al_{11}O_{16}N$ excited only by 185 nm radiation shows a decrease of 4%. Furthermore, the quantum efficiency (254 nm excitation) of this sample has decreased. This indicates that indeed the 185 nm radiation causes the decrease in spectral output.

The color points of the oxynitride phosphors are more to the green/white compared to BAM, which is the cause of the higher lumen output of these phosphors (despite the lower quantum efficiency). The maintenance tests of the single-component lamps show an increase of the color points (*X*, *Y*) resulting in a change of color

Table I. Quantum efficiency (*QE*) and UV-absorption (*A*) for 254 nm excitation of various Ba β-alumina phosphors doped with Eu ($x = 0.1$). ($Eu_{0.1(0.83+0.17y)}Ba_{0.9(0.83+0.17y)}Al_{11}O_{17.33-1.33y}N_y$) and commercial BAM as well as $Eu_{0.1}Ba_{0.9}MgAl_{10}O_{17}$. Data are shown for samples fired for 2 and 4 h at 1973 K.

Powder type	*QE* (%) 2 h	*A* (%) 2 h	*QE* (%) 4 h	*A* (%) 4 h
Commercial BAM	87	89	—	—
$Eu_{0.1}Ba_{0.9}MgAl_{10}O_{17}$	—	—	73	87
$y = 0$	83	81	85	84
$y = 0.17$	80	82	87	84
$y = 0.55$	82	79	85	89
$y = 1$	79	82	82	84

Table II. Quantum efficiency (*QE*), UV-absorption (*A*), and emission wavelength at maximum intensity ($\lambda_{em,max}$) at 254 nm excitation of various Eu-doped Ba β-alumina's (fired at 1973 K for 2 h) before and after oxidation test at 873 K for 10 min in air. The sample composition is $Eu_{x(0.83+0.17y)}Ba_{(1-x)(0.83+0.17y)}Al_{11}O_{17.33-1.33y}N_y$.

Sample *x*, *y*	*QE* (%)		*A* (%)		$\lambda_{em,max}$ (nm)	
	Before	After	Before	After	Before	After
0.05, 0	75	79	75	75	447	446
0.05, 1	78	72	73	73	456	453
0.10, 0	83	82	83	83	450	450
0.10, 1	76	73	84	83	456	456
0.15, 0	77	76	88	88	456	456
0.15, 1	80	74	87	87	456	456
Commercial BAM	87	86	89	89	451	451

Table III. Short-term depreciation (combined 185 and 254 nm) of various Eu-doped Ba β-alumina's fired at 1973 K for 2 h.

$Eu_{x(0.83+0.17y)}Ba_{(1-x)(0.83+0.17y)}Al_{11}O_{17.33-1.33y}N_y$	*STD* (%)
$x = 0.05$, $y = 0$	0.2
$x = 0.05$, $y = 1$	5.0
$x = 0.10$, $y = 0$	1.2
$x = 0.10$, $y = 0.17$	1.7
$x = 0.10$, $y = 0.55$	2.1
$x = 0.10$, $y = 1$	3.2
$x = 0.15$, $y = 1$ (only 185 nm)	4.0
Commercial BAM	0.0

S0013-4651(98)05-045-9 CCC: $7.00

Table IV. Color coordinates (*X*, *Y*) and lumen output of single component TL-lamps with oxynitride phosphors ($Eu_{0.925x}Ba_{(1-x)0.925}Al_{11}O_{16.59}N_{0.55}$) and commercial BAM.

	0 h		40 h		80 h	
Sample	*X*/*Y*	Lumen	*X*/*Y*	Lumen	*X*/*Y*	Lumen
$x = 0.10$	0.1821/0.1876	240	0.1835/0.1910	223	0.1839/0.1929	156
$x = 0.15$	0.2012/0.2477	318	0.2026/0.2498	282	0.2026/0.2514	196
Comm. BAM	0.1593/0.0873	159	0.1591/0.0899	137	0.1590/0.0907	95

toward green/white luminescence (Table IV). Also the lumen output decreases in time. To take into account the influence of the observed shift in the emission color, the lumen output was compared by taking the lumen/*Y* values. In Fig. 12 the lumen/*Y* values are shown as function of the operation time. The commercial BAM phosphor shows the highest lumen/*Y* output but also the strongest degradation. Therefore, the difference in lumen/*Y* output between BAM and the oxynitride phosphors becomes less for longer operation times.

From the emission spectrum measured for the single-component fluorescent lamp (Fig. 13) the CRI and lumen output of a tricolor lamp were calculated using these materials as the blue-emitting phosphors. Y_2O_3:Eu was taken as the red and (Ce, Tb)$MgAl_{11}O_{19}$ as the green emitting phosphor as is the case in a commercial tricolor lamp (Philips/85 series, color $x = 345$, $y = 351$). The results are displayed in Table V. The emission spectra of tricolor fluorescent lamps as calculated with PHOCAL are depicted in Fig. 13. It is clear from this figure that the emission spectrum of a tricolor lamp using Eu-doped barium aluminum oxynitride as the blue-emitting compound

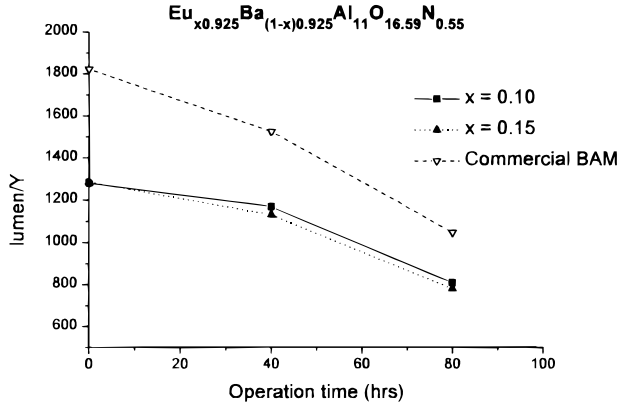

Figure 12. Lumen/*Y* output as a function of the operation time of single component TL lamps containing Eu-doped barium aluminum oxynitride as phosphor or commercial BAM.

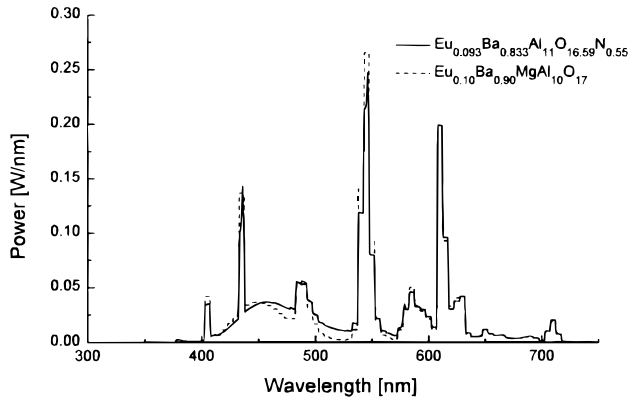

Figure 13. Calculated emission spectrum of a tricolor fluorescent lamp containing $Eu_{0.092}Ba_{0.833}Al_{11}O_{16.59}N_{0.55}$ or $Eu_{0.1}Ba_{0.9}MgAl_{10}O_{17}$ as blue-emitting phosphors.

results in an increased output in the range 450-530 nm compared to Eu-doped $BaMgAl_{10}O_{17}$.

It is clear that by using Eu-doped barium aluminum oxynitride phosphors the CRI can be increased to about 90 compared to 83 for BAM. The somewhat lower lumen output of these oxynitride phosphors compared to BAM can be ascribed to the lower quantum efficiency of these materials. To take this effect into account we have performed simulations based on the assumption that oxynitride phosphors actually tested in the fluorescent lamp have the same quantum efficiency as the maximum value achieved for the barium β-alumina oxynitride phosphors (Table I). This results in tricolor lamps with a calculated lumen output almost equal (88 lm/W) to tricolor lamps with BAM as blue-emitting phosphor (89 lm/W) while the color rendering index improves. A possible improvement in color rendering index without loss in lumen output was predicted by Yamamoto et al.[44] for blue-emitting phosphors by shifting the emission wavelength more to 480 nm. So it can be stated that novel Eu-doped Ba β-alumina oxynitrides are very interesting materials for use as blue-emitting phosphors in tricolor fluorescent lamps.

Conclusions

Novel Eu-doped barium aluminum oxynitride phosphors with the β-alumina-type structure were prepared by solid-state reactions. As expected, the *c*/*a* ratio of the β-alumina-type unit cell of these materials decreases with increasing nitrogen and europium content. The oxynitride phosphors show two emission bands for 254 nm excitation, similar to Eu-doped Ba aluminate phase I. The maximum quantum efficiency of the oxynitride phosphors is about 85-90% just like commercial BAM. The nonoptimized oxynitride phosphors are more sensitive to oxidation at 873 K and to short-term depreciation compared to Eu-doped Ba aluminate phase I and commercial BAM. However, the maintenance of the oxynitride phosphors is better compared with commercial BAM. The oxynitride materials are very attractive for use as a blue-emitting phosphor in tricolor fluorescent lamps, since the CRI of these tubes increases with preservation of a high lumen output.

Acknowledgment

The authors would like to thank Slobodan Markovski for making the SEM pictures and Dick van de Voort (Philips Lighting) for his help with the luminescence measurements, calculations, and discussions.

Table V. Simulated performance of a tricolor fluorescent lamp as a function of the blue-emitting phosphor. The composition of the oxynitride phosphor is $Eu_{0.925x}Ba_{(1-x)0.925}Al_{11}O_{16.59}N_{0.55}$.

Sample	Calculated CRI	Calculated lumen output (lm/W)	Calculated lumen output (lm/W)
Oxynitride $x = 0.10$	89	82[a]	88[b]
Oxynitride $x = 0.15$	91	83[a]	88[b]
Commercial BAM	83	89	

[a] Based on real quantum efficiency measured for these phosphors.
[b] Based on maximum quantum efficiency achievable for these phosphors.

S0013-4651(98)05-045-9 CCC: $7.00

Eindhoven University of Technology assisted in meeting the publication costs of this article.

References

1. M. Koedam and J. J. Opstelten, *Lighting Res. Technol*., **3**, 205 (1971).
2. W. A. Thornton, *J. Opt. Soc. Am*., **61**, 1155 (1971).
3. J. M. P. J. Verstegen, D. Radielovic, and L. E. Vrenken, *J. Electrochem. Soc*., **121**, 1627 (1971).
4. B. M. J. Smets, *Mater. Chem. Phys*., **16**, 283 (1987).
5. G. Blasse and B. C. Grabmaier, *Luminescent Materials*, Springer-Verlag, Berlin (1994).
6. A. L. N. Stevels and A. D. M. Schrama-de Pauw, *J. Electrochem. Soc*., **123**, 691 (1976).
7. F. Haberey, G. Oehlschlegel, and K. Sahl, *Ber. Dtsch. Keram. Ges*., **54** (11), 373 (1977).
8. F. P. F. van Berkel, H. W. Zandbergen, G. C. Verschoor, and D. J. W. Ijdo, *Acta Crystallogr. C*, **40**, 1124 (1984).
9. N. Iyi, Z. Inoue, S. Takekawa, and S. Kimura, *J. Solid State Chem*., **52**, 66 (1984).
10. G. Bartels, D. Mateika, and J. M. Robertson, *J. Cryst. Growth*, **47**, 414 (1979).
11. N. Iyi, S. Takekawa, Y. Bando, and S. Kimura, *J. Solid State Chem*., **47**, 34 (1983).
12. S. Kimura, E. Bannai, and I. Shindo, *Mater. Res. Bull*., **17**, 209 (1982).
13. A. Kahn, T. Gbehi, J. Théry, and J.-J. Legendre, *J. Solid State Chem*., **74**, 295 (1988).
14. G. Groppi, F. Assandri, M. Bellotto, C. Cristiani, and P. Forzatti, *J. Solid State Chem*., **114**, 326 (1995).
15. D. Mateika and H. Laudan, *J. Cryst. Growth*, **46**, 85 (1979).
16. M. Machida, K. Eguchi, and H. Arai, *J. Am. Ceram. Soc*., **71**, 1142 (1988).
17. M. Machida, K. Eguchi, and H. Arai, *J. Catal*., **103**, 385 (1987).
18. M. Machida, K. Eguchi, and H. Arai, *Chem. Lett*., 767 (1987).
19. M. Machida, K. Eguchi, and H. Arai, *Bull. Chem. Soc. Jpn*., **61**, 3659 (1988).
20. P. E. D. Morgan and T. M. Shaw, *Mater. Res. Bull*., **18**, 539 (1983).
21. T. Gbehi, D. Gourier, J. Théry, and D. Vivien, *J. Solid State Chem*., **83**, 340 (1989).
22. J. M. P. J. Verstegen and A. L. N. Stevels, *J. Lumin*., **9**, 406 (1974).
23. C. R. Ronda and B. M. J. Smets, *J. Electrochem. Soc*., **136**, 570 (1989).
24. B. M. J. Smets, J. Rutten, G. Hoeks, and J. G. Verlijsdonk, *J. Electrochem. Soc*., **136**, 2119 (1989).
25. B. M. J. Smets and J. G. Verlijsdonk, *Mater. Res. Bull*., **21**, 1305 (1986).
26. J. M. P. J. Verstegen, *J. Electrochem. Soc*., **121**, 1623 (1974).
27. A. L. N. Stevels. *J. Lumin*., **17**, 121 (1978).
28. G. Roth and G. Herzog, *Wiss. Z. Ernst-Moritz-Arndt-Univ. Greifswald*, **36**, 3 (1987).
29. T. R. N. Kutty and M. Nayak, *Mater. Res. Bull*., **30**, 325 (1995).
30. D. Nötzold, G. Herzog, and G. Roth, *Z. Phys. Chemie*, **271**, 715 (1990).
31. M. Tamatani, *Jpn. J. Appl. Phys*., **31**, 950 (1974).
32. S. Ekambaram and K. C. Patil, *J. Alloys Compd*., **248**, 7 (1997).
33. S. R. Jansen, H. T. Hintzen, and R. Metselaar, *J. Mater. Sci. Lett*., **15**, 794 (1996).
34. S. R. Jansen, H. T. Hintzen, and R. Metselaar, *J. Solid State Chem*., **129**, 66 (1997).
35. Chr. Meyer and H. Nienhuis, *Discharge Lamps*, Kluwer Technische boeken, Deventer, The Netherlands (1988).
36. S. R. Jansen, H. T. Hintzen, and R. metselaar, in *Proceedings of 4th Conference on Euro-Ceramics. Basic Science-Developments in Processing of Advanced Ceramics Part II*, C. Galassi, Editor, p. 353, Gruppo Editoriale Faenza Editrice S.p.A. Italy (1995).
37. R. D. Shannon, *Acta, Crystallogr. A*, **32**, 751 (1976).
38. S. R. Jansen, J. W. de Haan, L. J. M. van de Ven, R. Hanssen, H. T. Hintzen, and R. Metselaar, *Chem. Mater*., **9**, 1516 (1997).
39. S. R. Jansen, H. T. Hintzen, K. S. Knight, and R. Metselaar, To be published.
40. J. W. H. van Krevel, H. T. Hintzen, R. Metselaar, and A. Meijerink, *J. Alloys Compd*., **268,** 272 (1998).
41. S. R. Jansen, J. van Deelen, H. T. Hintzen, A. Meijerink, and R. Metselaar, To be published.
42. J. W. T. Vrugt, *Philips Res. Rep*., **20**, 23 (1965).
43. X. H. Wang, A. M. Lejus, and D. Vivien, *J. Am. Ceram. Soc*., **73**, 770 (1990).
44. T. Yamamoto, K. Iwama, and Y. Watarai, *J. Light Vis. Env*., **6**, 7 (1982).